Non-self-sustained oscillators effect entrainment flexibility of mammalian SCN across four models

Douglas Abrams[1] , Victoria A. Chistolini[1] , Jay Moore[1] , Zhuofan Zhang[1]
[1]Colby College Department of Computer Science, 04901

The Suprachiasmatic Nucleus (SCN) regulates a broad array of physiological functions in mammals. The mammalian SCN is made up of two regions, the ventro-lateral (VL) region and the dorso-medial (DM) region, and two oscillator types, self-sustained oscillators, which oscillate without external signaling, and non-self-sustained oscillators, which do not oscillate without external signaling. In this study, we investigate how the proportion of non-self-sustained neurons in the mammalian VL SCN and the mammalian DM SCN impact mammalian SCN entrainment by replicating the simulations of Gu et al. (*Nature,* 2016) in four different models of the mammalian SCN. While Gu et al. suggest that non-self-sustained oscillators hinder SCN entrainment in the VL and aid SCN entrainment in the DM, the models tested here reveal that, while DM entrainment is aided by non-self-sustained cells, VL entrainment is not hindered by non-self-sustained cells.

1 INTRODUCTION

In mammals, the suprachiasmatic nucleus (SCN) controls circadian rhythms regulating numerous physiological activities through cyclical gene expression [2]. The regulating rhythms of SCN cells are, themselves, regulated by both intrinsic cellular rhythms and extrinsic environmental rhythms. For different species, rhythmic patterns Free Running Periods (FRPs) and Lower Limit of Entrainment (LLEs) vary by the availability of intrinsic and extrinsic signals [1]. LLE is the shortest day/night cycle that the SCN is able to synchronize to, and represents the entrainment range of the SCN. FRP is the intrinsic period of the oscillators in the absence of environmental cue.

The SCN contains two regions: the ventro-lateral (VL) region, which makes up about 25% of the SCN and responds to extrinsic signaling, and the Dorso-Medial (DM) region, which makes up about 75% of the SCN and does not respond to extrinsic signaling [1]. In both regions, a minority of neurons with self-sustained oscillations drive the rhythm of SCN, while the rest, non-self-sustained neurons, aid in SCN entertainment, providing greater synchronization flexibility to the SCN [1].

Gu et al. (2016) explore the effects of the proportion (p) of non-self-sustained oscillators in both the VL and the DM SCN on the FRP and the LLE of the SCN using the Poincaré model to simulate the SCN. Their main result consists of three sets of simulations.

Simulation 1 shows that p does not affect SCN FRP when the SCN does not receive extrinsic signaling, but that it increases SCN LLE when the SCN receives extrinsic signaling.

Simulation 2 examines the effect of p on SCN entrainment to an extrinsic 23.6 hour rhythm when the SCN is modeled with both VL and DM regions. The first part of the simulation shows that the SCN entrains to an extrinsic signal when p is 0. The second part of the simulation shows that the SCN does not entrain to an extrinsic rhythm when the VL contains

70% non-self-sustained cells. In the last part of the simulation, Gu et al. show that the SCN entrains to an extrinsic signal when the DM SCN is composed of 70% non-self-sustained cells.

Simulation 3 shows that non-self-sustained cells decrease LLE when present in the VL, but increase LLE when present in the DM.

In this study, we attempt to recreate the findings of the three simulations discussed above using four different models of the mammalian SCN: the Poincare model [1] the Leloup-Goldbeter 16-stage model [3], the Gonze model [2], and the Phase-Amplitude model [4].

2 RESULTS

We examined the impact of the proportion of non-self-sustained oscillators in the SCN (p) on SCN entrainment in all four models of the mammalian circadian clock. We first generated parameter set libraries of non-self-sustained and self-sustained oscillators for the Gonze and Goldbeter models. Descriptive statistics of those libraries were then calculated (Fig. 2.0).

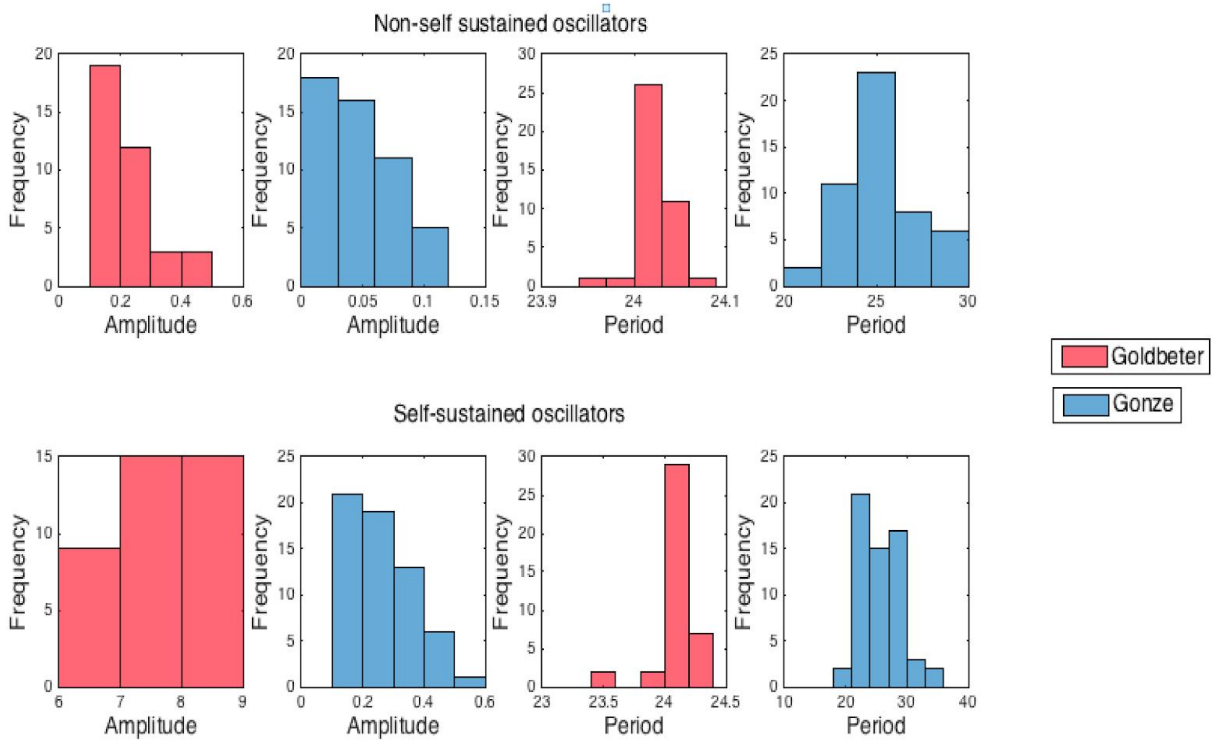

FIGURE 2.0. Descriptive statistics of the parameter libraries were calculated for both non-self-sustained and self-sustained oscillators for both the Gonze and Goldbeter models. In both libraries, the distribution of periods was similar across non-self-sustained and self-sustained cells, although the Gonze model's library had higher periods than the Goldbeter model in both non-self-sustained and self-sustained parameter sets

For both the Gonze and Goldbeter libraries, the distribution of periods was similar across non-self-sustained and self-sustained cells, although the Gonze model's library had higher periods than the Goldbeter model in both non-self-sustained and self-sustained parameter

sets (Fig. 2.0). Similarly, the parameter library of the Gonze model had a consistent distribution across non-self-sustained and self-sustained cells (Fig. 2.0). On the other hand, the library for the Goldbeter model has drastically higher amplitudes for self-sustained cells than for non-self-sustained cells (Fig. 2.0).

We then examined the effect of *p* on SCN FRP when the SCN does not receive external signaling at three levels of intra-SCN signaling (*g*). (Fig. 2.1A).

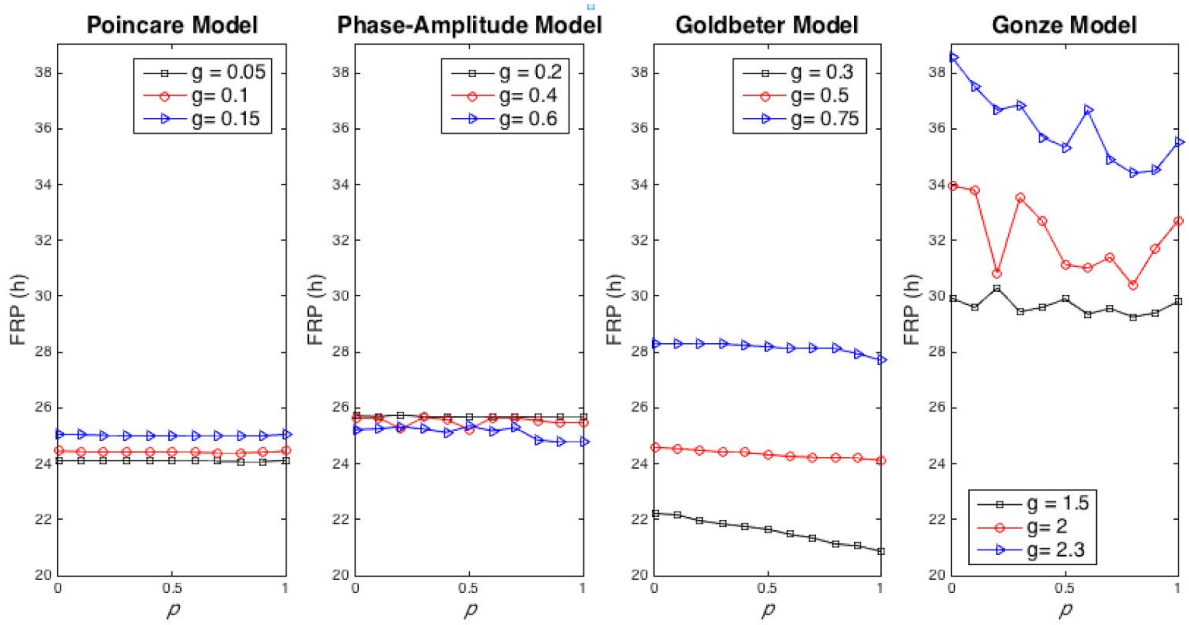

Figure 2.1A. For the four models, Free Running Periods were calculated for simulations in constant darkness across a range of non-self-sustained SCN proportions and three levels of coupling intensity (g), where the lowest level of g represented the weakest coupling strength. All models except for the Gonze model had relatively constant FRPs across all non-self-sustained proportions. The Gonze model's FRP values to not follow any discernible pattern.

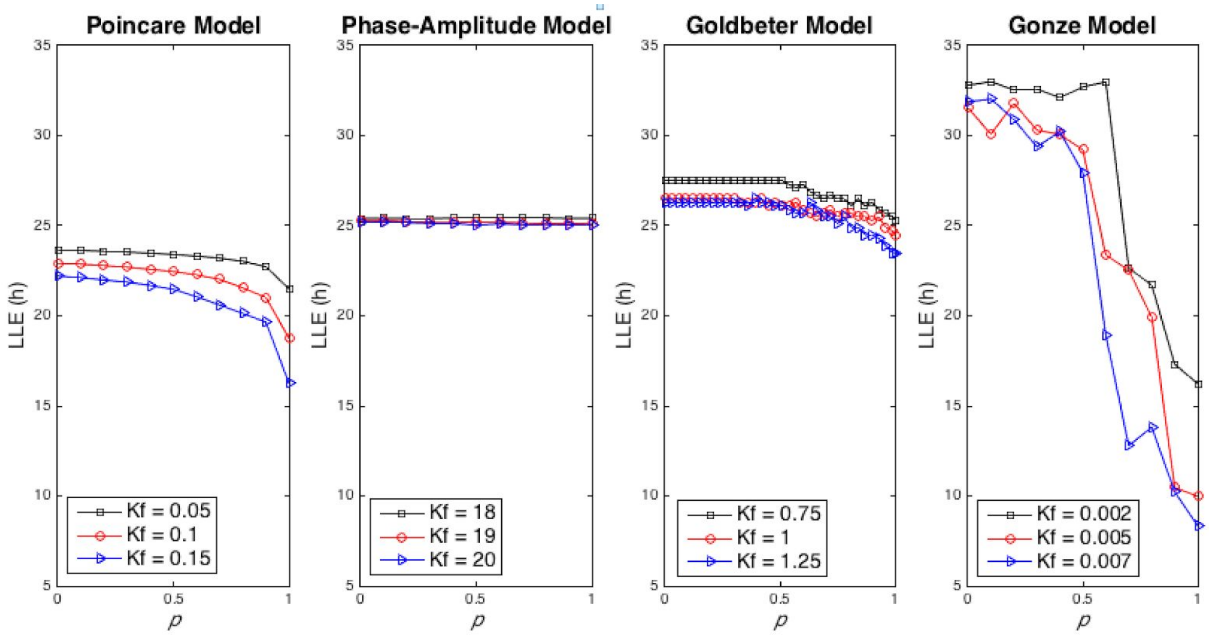

Figure 2.1B. Lower limit of entrainment (LLE) of each SCN model was calculated with different proportions of non-self-sustained cells across three levels of light intensity (Kf), where the lowest Kf value represented the weakest light intensity. For each model, coupling strength (g) was set to the "medium" value used in Fig. 2.1A. The LLE of all models except Phase-Amplitude decreased dramatically at higher levels of p. LLE did not change for eh Phase-Amplitude model at different levels of p.

In all the models except for the Gonze model, the FRP of the SCN did not change with increasing values of *p* across all levels of coupling strengths. In the Gonze model, FRP changed significantly with varying levels of *p,* although its changes did not follow any clear pattern (Fig. 2.1A). We then tested the impact of *p* on SCN entrainment, as measured by SCN LLE, when SCN cells receive external signaling at three different levels of external signaling (*Kf*) (Fig. 2.1B).

Strikingly, we found that, in all models but the Phase-Amplitude model, LLE increased when *p* increased at all *Kf* levels (Fig. 2.1B). In the Phase-Amplitude model, SCN LLE stayed the same as *p* increased (Fig. 2.1B)

Next, we examined the impact on entrainment by *p* to the SCN when the SCN was simulated with both a VL and a DM region (Fig. 2.2A, B, C). First we looked at how well the SCN could entrain to an external signal of 23.6 hours when the SCN did not contain non-self-sustained cells by plotting the mean concentration of *per* mRNA in VL SCN cells and in DM SCN cells (Fig. 2.2A). Across all four models, the rhythm of *per* mRNA oscillations in both the VL and the DM stayed the same over time, suggesting entrainment (Fig. 2.2A). In Fig. 2.2B, we looked at the effect of a high level of *p* in the VL (70%) on SCN entrainment to the same external signal (Fig. 2.2B).

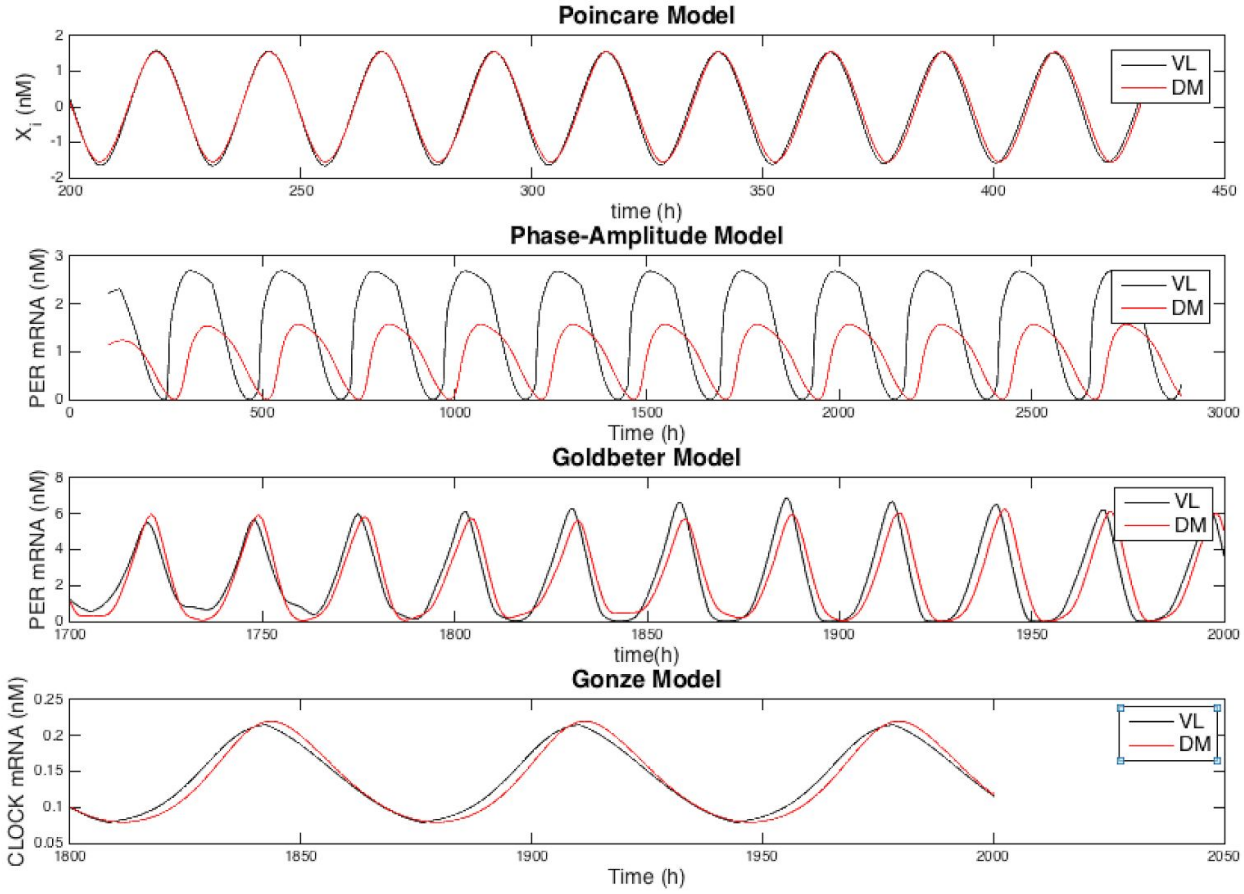

2.2A The evolutions in time of neuronal oscillators, when all the cells are self-sustained. For all models, the same coupling strengths and cell numbers were used as in Fig. 2.1A and Fig. 2.1B. In all models, both DM and VL cells entrained.

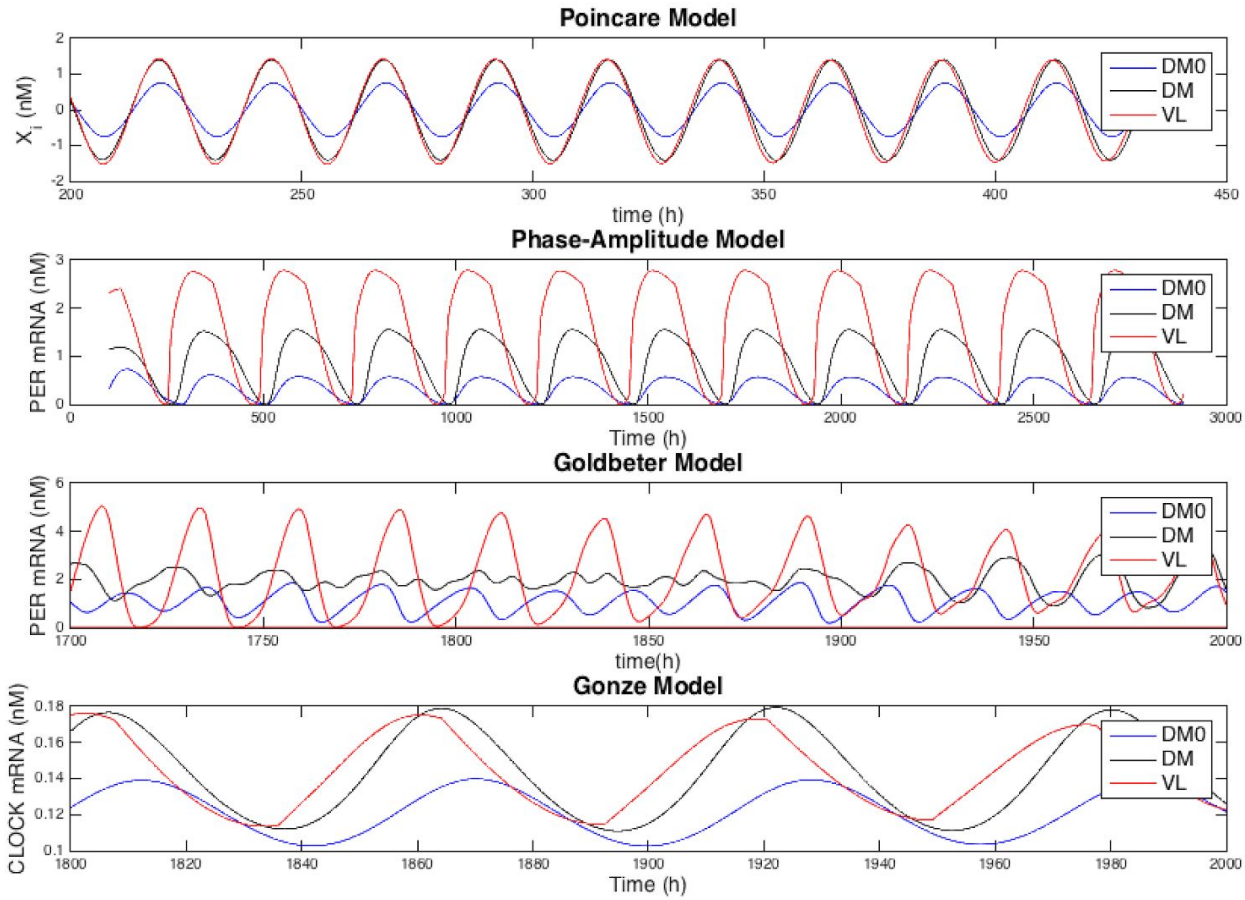

Figure 2.2B. The evolutions in time of neuronal oscillators when the intrinsic amplitudes R in 70% of VL neurons are equal to 0 (PVL=0.7) and when the extrinsic entrainment rhythm (T cycle) is set to 23.6. For all models, the same coupling strengths and cell numbers were used as in Fig. 2.1A and Fig. 2.1B. In all models but Goldebeter, the different cell populations entrained.

In all of the models except for the Goldbeter model, entrainment remained at high levels with the introduction of non-self-sustained cells (Fig. 2.2B). In the Goldbeter model, however, the mean phases of the different SCN regions shifted over time, suggesting low levels of entrainment (Fig. 2.2B). Finally, we examined SCN entrainment to an external signal when the DM contained 70% non-self-sustained cells (Fig. 2.2C). All models showed high levels of entrainment (Fig. 2.2 C).

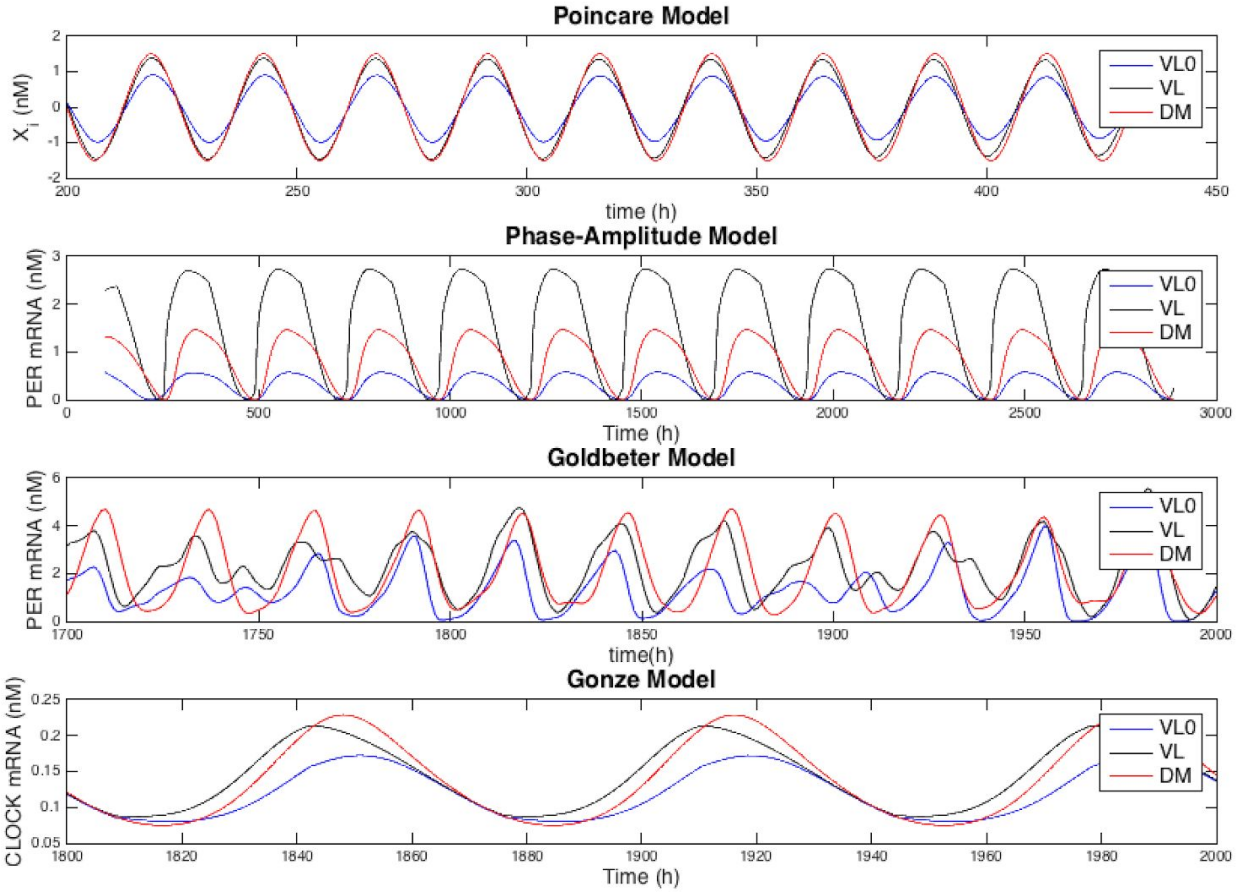

Figure 2.2C. The evolutions in time of neuronal oscillators, when the intrinsic amplitudes R in 70% of DM neurons the amplitudes R are equal to 0 (PDM =0.7). For all models, the same coupling strengths and cell numbers were used as in Fig. 2.1A and Fig. 2.1B. In all models, the cell populations entrained.

In Fig. 2.3A and B, we examine the effect of non-self-sustained cells on entrainment flexibility in both the VL SCN (A) and in the DM SCN (B). In all four models, non-self-sustained cells did not affect entrainment range (measured by LLE) when they were placed within the VL SCN (Fig 2.3A). Although the LLE did change with *p* in the Goldbeter and Gonze models, the changes did not follow any discernible pattern (Fig. 2.3A).

On the other hand, non-self-sustained cells greatly decreased LLE and increased the entrainment range when placed within the DM SCN in all models but the Phase-Amplitude model (Fig. 2.3B). In the Phase-Amplitude model, LLE varied unpredictably with *p* (Fig. 2.3B).

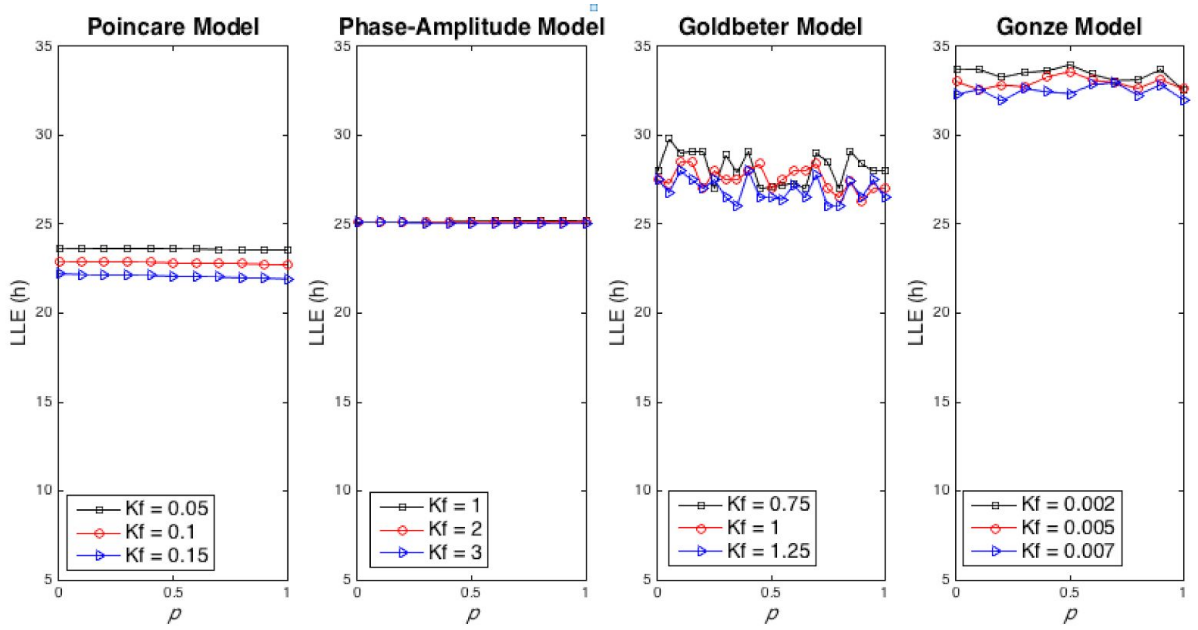

Figure 2.3A. Lower limit of entrainment of each SCN model with different proportion of non-self-sustained cells in VL region, assuming all cells in DM are self-sustained. Light intensity K_f varies among weak, medium, and strong for each model, while the coupling strength g is the middle value, as in Fig. 2.1B. In all 4 models, the proportion of non-self-sustained cells in VL did not affect the entrainment range (measured by LLE) in any obvious pattern.

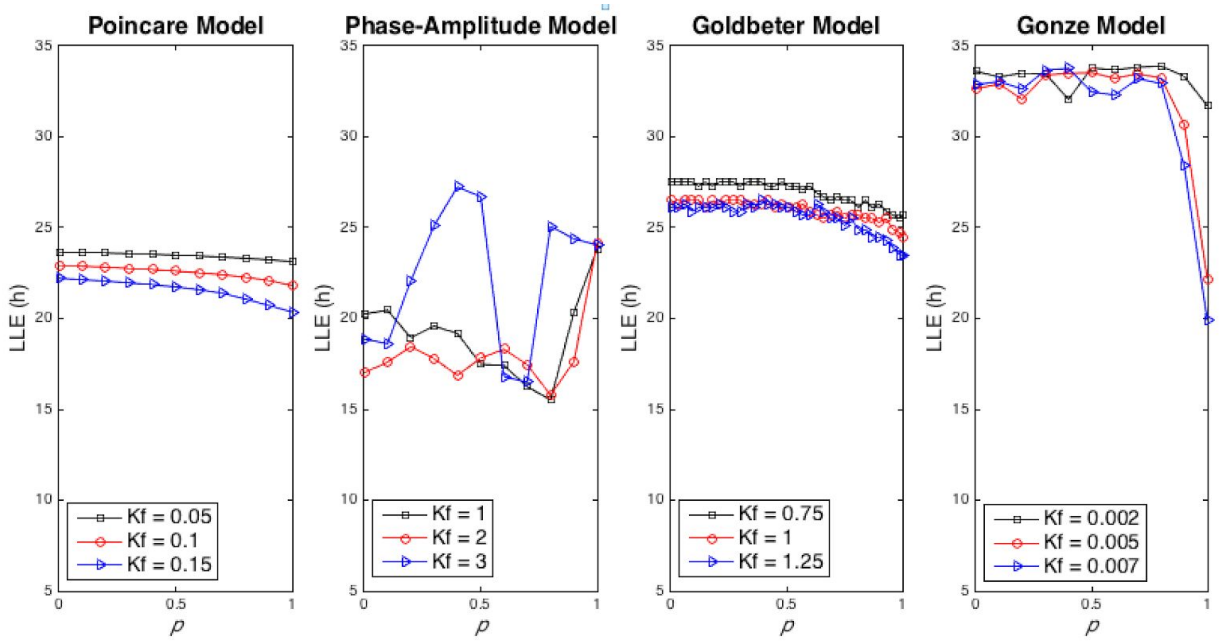

Figure 2.3B. Lower limit of entrainment of each SCN model with different proportion of non-self-sustained cells in DM region, assuming all cells in VL are self-sustained. Light intensity K_f varies among weak, medium, and strong for each model, while the coupling strength g is the middle value, as in Fig. 2.1B. In the Phase-Amplitude model, LLE varied unpredictably with p, the proportion of non-self-sustained cells in DM, while all other models showed decreased LLE with increasing p.

3 DISCUSSION

3.1 Replicating key results

The Goldbeter, Gonze, Poincaré and Phase-Amplitude models were able to validate many figures and results in Gu et al.

The features and organizations of these models varied highly (Sections 4.01 to 4.04). Despite these differences, all the models qualitatively matched basic behaviours of the circadian clock. 1) Strong oscillators maintained their period in constant darkness (Figure 4.2). 2) Weak oscillators were able to be entrained by stronger oscillators (Figure 4.2) and strong light signal strength (Figure 2.1B, 2.3B). Modeling DM and VL tissue types was also adaptable to all four models (Section 4.6).

Figure 2A, Gu et al. shows that VL entrains DM with only self-sustained cells. In Figure 2.2A, all four of our models display constant phase differences just as expected. Figure 2.2C also displays constant phase difference between the VL and DM cells. This shows that entrainment of DM by VL is strong when DM has damped cells.

Gu et al. claim that proportions of non-self-sustained oscillators in both DM and VL tissues affect entrainment (Figure 1 and Figure 3, Gu et al., 2016). High proportions of non-self-sustained DM cells made the model very sensitive to entrainment (Gu et al., 2016). This result is best replicated by the Gonze and Poincaré models, although Goldbeter reproduces a muted version of the trend (Figure 2.1B, 2.3B). However, the Phase-Amplitude model shows no change in its LLE when higher proportions of damped oscillators are simulated.

We were unable to replicate the impact of damped cells in the VL tissue in decreasing LLE of the models (Figure 3A, Gu et al., 2016). For all models, the proportions of damped cells has no effect on the LLE (Figure 2.3A).

3.2 Model-specific characteristics drive key results

Model sensitivity played a central role in this investigation and can describe the varied outcomes between models of our LLE analysis (2.1B and 2.3B). Highly insensitive models like Phase-Amplitude did not entrain through mean coupling or light signaling (Fig 2.1A and Fig 2.1B). As seen with a complex model like Goldbeter (Section 1.3), with 3 negative feedback loops, Figure 2.0 shows how narrow the sampling distribution of intrinsic periods are for the oscillators in the library, all oscillators have intrinsic periods in a range of 23-24.5h.

Conversely the Gonze model, which only has a single negative feedback loop making it highly sensitive, has periods that are approximately normally distributed with a mean of 25 and a standard deviation of approximately 3. Goldbeter, being highly insensitive, did not show as dramatic an entrainment range as did Gonze.

It is difficult to compare the Phase-Amplitude model to the other models, because its period is a model parameter. Mean field coupling is not strong enough for it to change the parameterized period. This insensitivity of the model periods is evident in Figure 2.1B, where the proportion of damped oscillators does not significantly perturb the LLE of the system. In Webb et al., a minimization algorithm was used to perturb kinetic parameters to generate damped oscillators [6].

Figure 2B, Gu et al. shows that there is a subtle phase difference between the VL and DM cells when damped cells are in the VL, meaning that the entrainment of the DM is weak. In

Figure 2.2B, the Poincare model shows the same subtle phase difference, and the Phase-Amplitude model shows strong entrainment of the DM by the VL. There are slight phase differences in the Gonze model between the non-self-sustained DM cells and VL, which is probably caused by position differences, but the overall entrainment is strong. However, the Goldbeter model has obvious phase differences, suggesting weak entrainment.

3.3 Validating the findings of Gu et al.

Overall we were able to demonstrate in four models that the high proportions of non-self-sustaining DM cells made the model very sensitive to entraintment, however we were unable to show the impact of non-self-sustaining cells in the VL on reduced system entrainment. Our results unanimously shows that damped cells in the VL had no effect on entrainment.

4 METHODS

4.0.1 Poincaré Model

In the Poincaré model, each cell contains two state variables that generate a generalized oscillation. With individual cells, the model uses an amplitude to decide if the oscillation is sustained through a positive feedback loop, or damped by a negative feedback loop. When cells are coupled together, the oscillation of each cell is sustained and synchronized by a mean field, in addition to a light input. The equations were first used by Abraham et al., and the results would be general enough [9].

4.0.2 Goodwin Oscillator

The Goodwin model is similar to the Poincaré model, in that it uses 3 state variables to generate generalized oscillations via a negative feedback loop. It simulates a simple control cycle, where the gene expresses a protein, and the protein induces a prohibitor for the gene. Besides the oscillation, the model also uses mean field coupling and light signal [3]. In our replication, we use the model modified by Gonze et al. in 2005.

4.0.3 Leloup-Goldbeter Model

Designed to simulate a sustained oscillation based on the intertwined relationship between multiple genes, the Leloup-Goldbeter model is a relatively accurate representation of the mammalian circadian clock. It contains 16 state variables and 73 parameters, to simulate 3 negative feedback loops together. It simulates coupling between cells via mean field and VIP (vasoactive intestinal peptide) signaling, which upregulates *per* mRNA transcription. The model can also generate damped oscillations by tweaking parameters, though it was not designed for studies on the effects from the proportion of non-self-sustained cells.

4.0.4 Phase-Amplitude Model

The Phase-Amplitude model describes multiple cells in a network. Each cell has a sinusoidal curve for the the levels of Period (*per*) mRNA. *per* mRNA encodes for the PER protein which regulates the cell's period. This model is different from the Poincaré, Goodwin and Goldbeter model because it does model the gene regulatory networks in the mammalian circadian clock. This model uses mean field coupling of vasoactive intestinal peptide (VIP)

for intercellular signaling. Light input speeds up the period and increases the amplitude of *per* mRNA productions. [5]

4.1 Creating damped vs sustained cells in different models

Our fundamental research question is about how the proportions of sustained and damped cells in the mammalian SCN affect entrainment ability. Thus it is essential that we explore how sustained and damped oscillators may be represented in the four different models used in our experiments. Figure 4.1 shows a graphical representation of a sustained oscillator versus a damped oscillator; sustained oscillators are able to maintain the same amplitude in constant darkness, while damped oscillators' amplitudes gradually decline significantly or fade out completely when there is no light input.

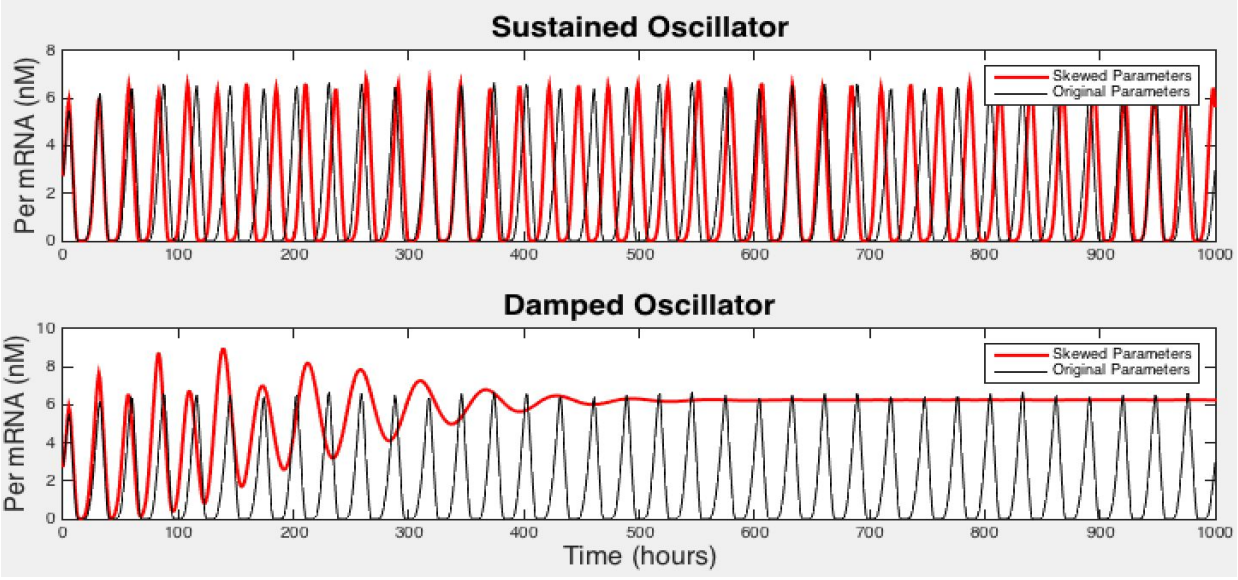

Figure 4.1. Comparison of a sustained oscillator (top) and damped oscillator (bottom) simulated in constant darkness.

In the Poincaré model three parameters control whether a cell is sustained or damped: relaxation parameter, intrinsic neuronal amplitude, and neuronal amplitude. A single parameter, R, is responsible for each cell's neuronal amplitude. Setting R = 0 produces a damped oscillator, while setting R = 1 results in a sustained oscillator.

. To simulate different cell types in the Phase-Amplitude model, we set steady state amplitudes for strong oscillators to 1.0 and weak oscillators to 0.1.

4.2 Libraries of cells

The Gonze and Goldbeter models do not have specific model parameters that result in damped or sustained behavior when tuned. Thus it is necessary to simultaneously perturb all model parameters by a random offset of the published parameter sets and then run the simulation and judge if an oscillator appears damped or sustained. Based on the visual classification of the simulation results of each parameter set, a library of sustained and damped cells can be created.

$$V_{perturbed} = |\frac{V}{200}(r + V)|$$

(equation 4.1)

The Goldbeter libraries were created by randomly perturbing the first 55 model parameters using equation 4.1. Cells were determined to be damped if the difference between the first peak and last peak in 1000 hours of simulation was large. The sustained library had 40 cells and the damped library had 40 cells.

Similarly, for the Gonze model, all parameters were perturbed by equation 4.2. Thus for each parameter we add an offset to the published parameter that is drawn randomly from a normal distribution with mean 1 and standard deviation 0.1. Simulation results from the models are classified as sustained and damped the same way as in the Goldbeter libraries. The finished sustained library had 60 cells and the damped library had 50 cells.

```
publishedParams(i) * normrand(1, 0.1)
```

(equation 4.2)

4.3 Network topology of cells

In the work done by Gu et al., all cells were connected to each other, in a network topology called mean field coupling. In mean field coupling, at each simulation time step, the current concentrations of clock mRNA produced by each cell is averaged over the number of cells in the network. The result, called VIP (vasoactive intestinal peptide), is sent back to all of the cells as a synchronization signal. The VIP synchronization signal helps cells that are lagging behind produce higher concentrations of clock mRNA to catch up.

The introduction of the VIP signal creates intercellular coupling, allowing for communication between cells. For the Gonze, Goldbetter and Poincaré model VIP is added to the X (clock mRNA) production equation. In the Phase-Amp model, since there are no equations specifically representing any biochemical molecules, a parameter η represents intercellular coupling.

4.4 Experiment 1A: determining coupling strength

In experiment 1A, we wanted to see if in constant darkness the average FRP of the system depends on the proportion of damped oscillators in the SCN, as shown in (Figure 1A, Gu et al.). We tested the relationship with networks of cells coupled weakly, moderately and strongly .

It is unclear what the magnitude of the additive effect on the model by VIP should be, or whether the raw average is sufficient to produce a noticeable synchronization response from the cells. In order to represent this uncertainty, we add a coupling strength coefficient, g, as an additional model parameter. In order to replicate experiment 1A, we needed to determine the values of g that produce weakly, moderately and strongly coupled network of cells for each model.

For the Poincaré model, 40(1-p) sustained and 40p damped cells, tested in 0.1 increments of p from 0 to 1, were used. The coupling strength coefficients g were defined in Gu et al. to be 0.05, 0.1 and 0.15.

For the Phase-Amplitude model, 169 sustained and 169 damped cells were simulated at p in {0,0.1,0.2,..1}. Since the model parameter η completely defines coupling strength in the model several values in {0, 0.05, 0.1, 0.15 ,...,1} were tried for η. Final η values were 0.2, 0.4 and 0.6.

For the Goldbeter model, 40 sustained and 40*p damped cells were simulated at p in {0,0.1,0.2,..1}. In order to determine coupling strength we relied on graphical evidence of syncrony at different values of g. Using 12 damped and 12 sustained cells, we found a g_1 that led to a very well synchronized network, g_2 that led to very weak evidence of synchronization, and a moderate

value $g_3 = (g_1+g_2)/2$. Final g values, shown in Figure 2.2, were $g_1 = 0.7$, $g_2 = 0.01$, and $g_3 = 0.3$.

For the Gonze model, we used 100 cells, p*100 damped and (1-p)*100 sustained cells, such that p is in {0, 0.1 ,0.2 ,.., 1} for our simulation. We used graphical evidence, like in the Goldbeter model, to determine g_1, strong coupling, g_2 moderate coupling and g_3, weak coupling. Figure 2.3 shows results of simulating 20 damped and 20 sustained cells at different g values. Initially we thought 1.0 was a good lower bound on g. However, in Figure 2.3, when g=1.0, the average FRP is actually inconsistent. Between hours 640 and 680, the average FRP flat lines and then resumes oscillation. Due to this inconsistent average FRP we decided to use $g_1 = 1.5$, $g_2 = 2.0$ and $g_3 = 2.3$ in the experiment.

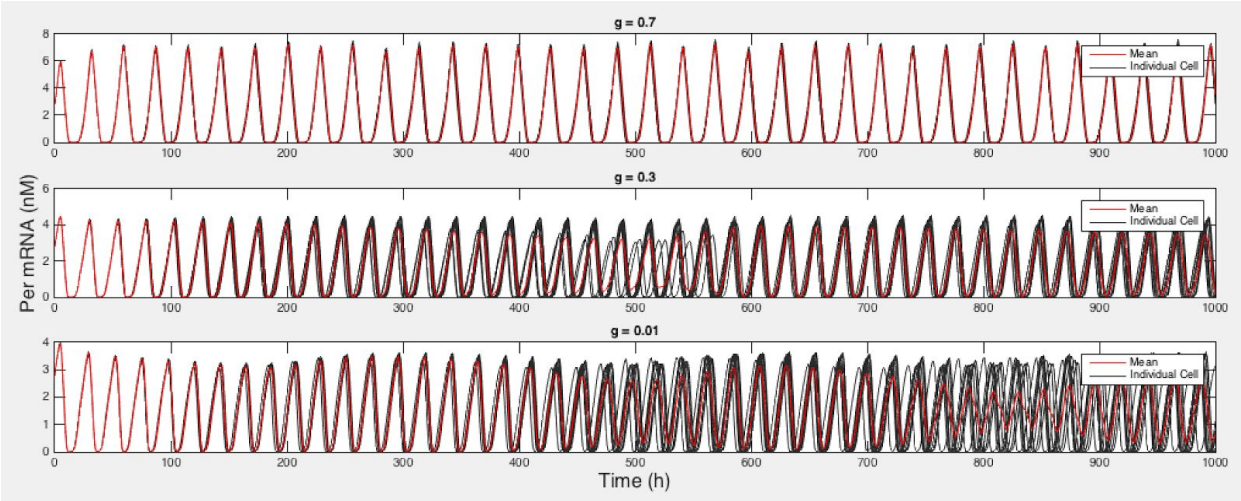

Figure 4.2 shows graphical evidence of the strong synchrony achieved at g = 0.7, moderate synchrony achieved at g = 0.3 and weak syncrony at g = 0.01.

4.5 Experiment 1B: determining light signal strength

Experiment 1B tests the impact of the proportion of damped oscillators on the lower level of entrainment of the system. All cells are sensitive to the light pulse which drives entrainment. For all models the same number of sustained and damped cells were used as in experiment 1A. In all models the light pulse was simulated cyclically for a period length of t hours, such that for t/2 hours l_{sig} =1 is added to the model X equation that represents activation of the clock gene, and for the other t/2 hours l_{sig} = 0 is added to the X equation, except for the Phase-Amplitude model where l_{sig} is represented in the model by a saturated light signal.

Since we were seeking the LLE, we wanted to find the lowest t to which the system can entrain. The minimum value of t is found by starting with t equal to the FRP in constant darkness, and then trying lower values of t and seeing if the average FRP gets smaller than t. If the average FRP becomes larger than t, then the system has failed to entrain to this t, and our maximum t is the previous value.

Similar to section 4.4 where we were not certain what the magnitude of the VIP should be, we also do not know what the magnitude of l_{sig} should be. Thus we needed to determine magnitude coefficients for l_{sig}, k, similar to how we found g.

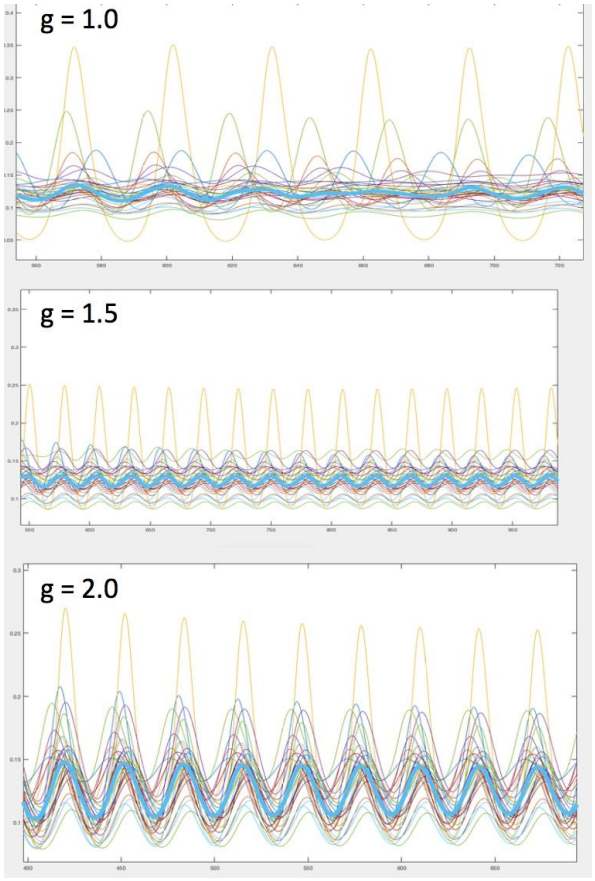

Figure 4.3 shows strong synchrony at g=1, moderate synchrony at g=1.5 and strong syncrony at g=2.0. The x-axis represents simulation time in hours and clock mRNA concentration on the y-axis.

For the Poincaré model, the published k values in Gu et al. were used.

For the Phase-Amplitude model, the values of k were given to us by Stephanie R. Taylor.

For the Goldbeter and Gonze models, k was derived graphically similar to the derivation of g in 4.4 such that k_1 for a weak signal allowed a very narrow amount of entrainment, while k_2 for a strong signal allowed high model flexibility and k_3 for moderate flexibility was the midpoint of these two extremes. For Goldbeter, $k_1 = 0.75$, $k_2 = 1.25$ and $k_3 = 1$.

For the Gonze model, it was easy to define k_1, but the model was so sensitive that it was possible to pick a k_2 that would essentially allow a system with 50-50 sustained-damped to entrain to any t-cycle. Thus we picked our strong k_2 so it would be closer to k_1. We found that $k_1 = 0.002$, $k_2 = 0.007$, $k_3 = 0.005$.

4.6 Experiment 2: simulating VL and DM cells

In order to simulate VL cells which are light sensitive and DM cells which are light insensitive, for all four models we created a vector called cell_type, containing 1 if the cell type was a VL cell or 0 if the cell type was a DM cell. Then we multiplied l_{sig} (section 4.5) by the cell_type vector to regulate which cell would receive input signal and which would not.

For experiment 2A, all VL and DM cells were sustained, with 25% of cells in the in the

VL and 75% of cells in the DM. In experiment 2B, 70% of VL cells were damped, while in 2C, 70% of DM cells were damped. For all three experiments the following settings were used:

For the Poincaré model the *t*_cycle was set to 23.6 hours, $k = 0.1$ and $g = 0.1$. We used 40 total cells in the simulation.

For the Phase-Amplitude model the *t*_cycle was set to 25.1 hours, $k = 1$ and $g = 0.2$. We used 169 total cells in the simulation.

For the Goldbeter model the *t*_cycle was set to 25.5 hours, $k = 1$ and $g = 0.1$. We used 40 total cells in the simulation.

For the Gonze model the *t*_cycle was set to approximately 34 hours (the FRP in constant darkness of the particular system is found and used as the *t*_cycle), $k = 0.005$ and $g = 2$. We use 100 total cells in the simulation.

4.7 Experiment 3: simulating VL and DM cells under light-dark cycle with damped cells

In experiment 3A, we were simulating the impact of changing the proportion of damped cells in the VL. In 3B, we simulated changing the proportion of damped cells in the DM.

For both 3A and 3B all models used 25% of total cells in the VL and 75% in the DM as well as the same settings for total number of cells, *t*_cycle, *k* and *g* from section 4.6.

5 SOURCES

1. Gu, C., Tang, M., Rohling, J. and Yang, H. (2016). The effects of non-self-sustained oscillators on the en-trainment ability of the suprachiasmatic nucleus. *Scientific Reports*, 6(1).
2. Reppert, S. and Weaver, D. (2002). Coordination of circadian timing in mammals. *Nature*, 418(6901), pp.935-941.
3. Gonze, D., Bernard, S., Waltermann, C., Kramer, A. and Herzel, H. (2005). Spontaneous Synchronization of Coupled Circadian Oscillators. *Biophysical Journal*, 89(1), pp.120-129.
4. Leloup, J. and Goldbeter, A. (2003). Toward a detailed computational model for the mammalian circadian clock. *Proceedings of the National Academy of Sciences*, 100(12), pp.7051-7056.
5. Taylor, S., Wang, T., Granados-Fuentes, D. and Herzog, E. (2016). Resynchronization Dynamics Reveal that the Ventral Entrains the Dorsal Suprachiasmatic Nucleus. *Journal of Biological Rhythms*, 32(1), pp.35-47.
6. Webb, A., Taylor, S., Thoroughman, K., Doyle, F. and Herzog, E. (2012). Weakly Circadian Cells Improve Resynchrony. *PLoS Computational Biology*, 8(11), p.e1002787.
7. Abraham, U., Granada, A., Westermark, P., Heine, M., Kramer, A., Herzel, H. (2010). Coupling governs entrainment range of circadian clocks. *Mol. Syst. Biol.* 6, pp.438.